Journal of Engineering Mathematics (2005) 52: 35–51
DOI 10.1007/s10665-004-3949-5

Initial response of a micro-polar hypoplastic material under plane shearing

ERICH BAUER
Institute of General Mechanics, Graz University of Technology, A-8010 Graz, Austria (erich.bauer@tugraz.at)

Received 18 March 2004; accepted in revised form 24 September 2004

Abstract. The behavior of an infinite strip of a micro-polar hypoplastic material located between two parallel plates under plane shearing is investigated. The evolution equation of the stress tensor and the couple-stress tensor is described using tensor-valued functions, which are nonlinear and positively homogeneous of first order in the rate of deformation and the rate of curvature. For the initial response of the sheared layer an analytical solution is derived and discussed for different micro-polar boundary conditions at the bottom and top surfaces of the layer. It is shown that polar quantities appear within the shear layer from the beginning of shearing with the exception of zero couple stresses prescribed at the boundaries.

Key words: granular materials, hypoplasticity, interface behavior, micro-polar continuum, plane shearing

1. Introduction

The objective of the present paper is to investigate the initial response of an infinite granular layer located between two parallel plates under plane shearing using a continuum approach. The grains of the dry and frictional material are assumed to be incompressible as usual in the constitutive modeling of granular materials like sand or powder. Consequently, the volume change of the void space equals the volume change of the granular body and the granular body with empty voids can be modeled based on a single-component continuum. For incompressible grains inelastic deformations of the granular body are caused by sliding and rotating of particles against each other. The slide and rotation resistance is mainly determined by the shape, size, and surface roughness of the particles, the packing density, the orientation of the contact planes and the pressure level. Constitutive models based on a local or so-called classical continuum fail to describe micro-polar properties of granular materials, which are evident when shear deformation takes place. For instance, in a ring shear apparatus [1] the displacement field across the height of a granular layer under shearing is nonlinear and related to the micro-rotations of particles, which are different from the macro-rotations. Under large monotonic shearing the deformation is located within a zone of a thickness that is approximately 10–20 grain diameters [2–5]. In order to model such properties, an expanded continuum theory which reflects certain changes in the micro-structure of the material is needed. Non-local continuum models are characterized by internal length scales, additional kinematic degrees of freedom and/or higher order deformation gradients as outlined for instance in [6, 7], [8, pp. 4–24], [9–12]. In the present paper a micro-polar or so-called Cosserat continuum within the framework of hypoplasticity is used, which allows relating the characteristic length to the mean grain size in a physically natural manner.

Originally, the concept of hypoplasticity was developed based on a local or so-called classical continuum [13, 14]. The term hypoplasticity was introduced by Dafalias [15] for a certain

type of hardening plasticity and was subsequently adopted for a class of nonlinear constitutive models of the rate type, which can be understood as a generalization of the theory of hypoelasticity [16,17]. In the present paper the hypoplastic concept as proposed by Kolymbas [13] is considered, which differs fundamentally from the concept of elastoplasticity, as no decomposition of the rate of deformation into reversible and irreversible parts is needed. Inelastic material properties are modeled in hypoplasticity with inherently nonlinear isotropic tensor-valued functions depending on the rate of deformation and the rate of curvature. For instance, in the case of a non-polar hypoplastic material, the evolution of the stress tensor is represented by the sum of a tensor function which is linear in the rate of deformation, and a tensor function which is nonlinear in the rate of deformation. A flow rule and a stress limit condition are not described by separate functions in hypoplasticity but instead are included in the evolution equation for the state quantities. The advantage of the hypoplastic concept lies not only in the formulation of the constitutive equation, but also in an easy adaptation of the constitutive constants to experiments. Within the last two decades various hypoplastic material models for frictional granular materials have been proposed, predominantly within the framework of a classical continuum; see *e.g.* [13,14,18–21]. A comprehensive review of the historical development, performance and limitation of hypoplastic models is given in [19,22–24]. Extensions of the local hypoplastic model with quantities which are relevant for a micropolar continuum, *i.e.,* rotational degrees of freedom in addition to translational degrees of freedom, non-symmetric shear stresses, couple stresses and the mean grain diameter as the internal length, are outlined in [25–31]. Both the non-polar hypoplastic model and the micropolar model were implemented into a finite-element program and applied to different practical problems; see *e.g.* [32–35].

Analytical solutions are rare and can only be derived for certain boundary-value problems using simplified versions of hypoplastic models as shown for a non-polar hypoplastic model by Hill [36] and for a micro-polar hypoplastic model by Bauer and Huang [37], Hunag [38, pp. 71–78]. The latter was the first analytical solution given for an infinite layer of a micropolar hypoplastic material at the onset of plane shearing. In the present paper this solution is extended to the full set of state quantities involved, and is discussed for different micro-polar boundary conditions. In contrast to earlier micro-polar hypoplastic versions by Tejchman and Gudehus [30] and Huang *et al*. [31], a simplified micro-polar hypoplastic model is employed for the present study, where the influence of the rate of deformation and rate of curvature is decoupled. In particular, the evolution equation for the non-symmetric stress tensor and the couple-stress tensor is described by tensor-valued functions which are nonlinear and homogeneous of first order only in the rate of deformation and the rate of curvature, respectively. Compared to earlier versions, an additional constitutive constant is included in the present model to refine the calibration of the volume-strain behavior.

The paper is organized as follows: In Section 2 the concept of hypoplasticity is briefly outlined for a non-polar continuum. Section 3 describes the extension to a micro-polar hypoplastic continuum which is used in Section 4 to model the plane shearing of an infinite granular layer under a constant vertical pressure. In Section 5 an analytical solution is derived for the initial response of the sheared layer and discussed for different micro-polar boundary conditions. Concluding remarks are presented in Section 6.

2. The concept of hypoplasticity

In the following the mechanical behavior of dry and cohesionless granular materials with simple grain skeletons [27] is considered under quasi-static and isothermal conditions. The

void-space between the grain skeleton is assumed to be empty and continuously connected. The ratio of the volume of the voids to the volume of solid particles is called the void ratio e, which is related to the bulk density ρ of the granular material as:

$$e = \frac{\rho_s}{\rho} - 1, \tag{2.1}$$

where ρ_s denotes the mass density of the solid grains. If the change of ρ_s under load can be neglected, the volume change of the granular material is determined by the volume change of the void space. With Equation (2.1) and $\rho_s = \text{constant}$ the balance relation of mass, *i.e.,* $\dot{\rho} + \rho \operatorname{div} \dot{\mathbf{x}} = 0$, can be rewritten as:

$$\dot{e} = (1 + e) \operatorname{div} \dot{\mathbf{x}}, \tag{2.2}$$

where $\dot{\mathbf{x}}$ denotes the mean field velocity of the grain assembly. It follows from relation (2.2) that the void ratio e is not an independent process variable, and that for an empty void space with $\rho_s = \text{constant}$ a granular body can be treated as a single-component continuum.

Within the framework of a classical hypoplastic continuum, the evolution of a stress state is described by an isotropic tensor-valued function $\mathbf{H}$ depending in the simplest case on the current Cauchy stress $\mathbf{T}$ and the symmetric part of the velocity gradient or so-called rate of deformation $\mathbf{D}$, *i.e.*, $\mathring{\mathbf{T}} = \mathbf{H}(\mathbf{T}, \mathbf{D})$. In order to specify the function $\mathbf{H}$, several requirements must be fulfilled which are based on basic continuum mechanics and on the general mechanical behavior of granular materials detected in experiments. For a rate-independent material behavior the function $\mathbf{H}$ must be positively homogeneous of first order in $\mathbf{D}$, *i.e.*, $\mathbf{H}(\mathbf{T}, \lambda \mathbf{D}) = \lambda \mathbf{H}(\mathbf{T}, \mathbf{D})$ holds for any scalar $\lambda > 0$. In order to describe an inelastic behavior, the function $\mathbf{H}$ must be a nonlinear function of $\mathbf{D}$, *i.e.*, $\mathbf{H}(\mathbf{T}, \mathbf{D}) \neq -\mathbf{H}(\mathbf{T}, -\mathbf{D})$. In hypoplasticity both the homogeneity of the first order in $\mathbf{D}$ and the nonlinearity in $\mathbf{D}$ are satisfied by a decomposition of the tensor function $\mathbf{H}(\mathbf{T}, \mathbf{D})$ into the sum of the following two parts [13]:

$$\mathbf{H}(\mathbf{T}, \mathbf{D}) = \mathcal{L}(\mathbf{T}) : \mathbf{D} + \mathbf{\Lambda}(\mathbf{T}) \, \|\mathbf{D}\| \, . \tag{2.3}$$

Herein the tensor function $\mathcal{L}(\mathbf{T}) : \mathbf{D}$ is linear in $\mathbf{D}$, and the tensor function $\mathbf{\Lambda}(\mathbf{T}) \, \|\mathbf{D}\|$ is nonlinear in $\mathbf{D}$ with respect to the Euclidean norm of $\mathbf{D}$, i.e. $\|\mathbf{D}\| = \sqrt{\mathbf{D} : \mathbf{D}}$. It is easy to prove that, with the basic concept of hypoplasticity in the form of the constitutive equation (2.3), inelastic material properties are modeled. For two particular strain rates $\mathbf{D}_a$ and $\mathbf{D}_b$ with the same norm, *i.e.*, $\|\mathbf{D}_a\| = \|\mathbf{D}_b\|$, but opposite principal directions, *i.e.*, $\mathbf{D}_b = -\mathbf{D}_a$, the corresponding responses of Equation (2.3) are $\mathbf{H}(\mathbf{T}, \mathbf{D}_a) \neq -\mathbf{H}(\mathbf{T}, \mathbf{D}_b)$. Therefore an inherently inelastic material behavior is described with a single constitutive equation and there is no need to decompose the deformation into elastic and plastic parts. Limit states are also included in the constitutive equation (2.3) for particular $\mathbf{T}$ and $\mathbf{D}$ fulfilling the condition: $\mathcal{L}(\mathbf{T}) : \mathbf{D} + \mathbf{\Lambda}(\mathbf{T}) \, \|\mathbf{D}\| = \mathbf{0}$; see *e.g.* [13,39]. For a refined modeling of the mechanical properties of granular materials the tensor functions $\mathcal{L}$ and $\mathbf{\Lambda}$ in (2.3) may also depend on additional scalar- and tensor-valued state variables. For instance, the influence of pressure and on the incremental stiffness can be taken into account by scaling $\mathcal{L}$ and $\mathbf{\Lambda}$ with a pressure-dependent stiffness factor and densityfactor [19,20,40,41]; rate-dependent properties can be introduced in the nonlinear part of the constitutive relation [42,43], and with additional structure tensors initial anisotropy [44,45], cohesion [46] and a so-called inter-granular strain [47] can be modeled. In order to also take into account particle rotation and couple stresses the non-polar constitutive relation (2.3) was extended to a micro-polar continuum [28,30,31], which is discussed in more detail in the next section.

3. Micro-polar hypoplastic model

In a micro-polar continuum, *e.g.* [8], the kinematics are characterized by the velocity vector $\dot{\mathbf{x}}$ and the micro-spin vector or so-called Cosserat spin vector $\dot{\boldsymbol{\omega}}^c$. The micro-spin tensor $\mathbf{W}^c$, the rate of deformation $\mathbf{D}^c$ and the rate of curvature $\mathbf{K}$ are defined as:

$$\mathbf{W}^c = -\boldsymbol{\epsilon}\,\dot{\boldsymbol{\omega}}^c\,, \quad \mathbf{D}^c = \mathbf{L} - \mathbf{W}^c\,, \quad \mathbf{K} = \operatorname{grad}\dot{\boldsymbol{\omega}}^c\,. \tag{3.1}$$

Herein the third-order tensor $\boldsymbol{\epsilon}$ denotes the permutation tensor. The velocity gradient $\mathbf{L} = \operatorname{grad}\dot{\mathbf{x}}$ in (3.1) is related to the macro-motion and can be decomposed into the symmetric part $\mathbf{D} = (\mathbf{L} + \mathbf{L}^T)/2$ and the skew-symmetric part $\mathbf{W} = (\mathbf{L} - \mathbf{L}^T)/2$. The definition of tensor $\mathbf{D}$ is the same as for the rate of deformation in a non-polar continuum. The macro-spin tensor $\mathbf{W}$ can also be represented by the rate of the macro-spin vector $\dot{\boldsymbol{\omega}}$, *i.e.*, $\mathbf{W} = -\boldsymbol{\epsilon}\,\dot{\boldsymbol{\omega}}$. Hence definition (3.1) for the rate of deformation can alternatively be written as

$$\mathbf{D}^c = \mathbf{D} + \mathbf{W} - \mathbf{W}^c. \tag{3.2}$$

Representation (3.2) indicates that, in the case where the macro-spin is equal to the micro-spin, *i.e.*, $\dot{\boldsymbol{\omega}} = \dot{\boldsymbol{\omega}}^c$, the rate of deformation $\mathbf{D}^c$ reduces to the tensor $\mathbf{D}$ of the classical non-polar continuum. The kinematic quantities $\mathbf{D}^c$ and $\mathbf{K}$ are associated with the stress tensor $\mathbf{T}$ and the couple-stress tensor $\mathbf{M}$ defined for the current configuration. For quasi-static processes the local-equilibrium equations read:

$$\operatorname{div}\mathbf{T} + \rho\,\tilde{\mathbf{b}} = \mathbf{0}, \tag{3.3}$$

$$\operatorname{div}\mathbf{M} - \boldsymbol{\epsilon} : \mathbf{T} + \rho\,\tilde{\mathbf{m}} = \mathbf{0}. \tag{3.4}$$

Herein ρ denotes the bulk density of the material, $\tilde{\mathbf{b}}$ and $\tilde{\mathbf{m}}$ represent the body force and body couple, respectively. Equation (3.4) indicates that the stress tensor in a micro-polar continuum is usually non-symmetric with the exception of states with $\operatorname{div}\mathbf{M} = 0$ and $\tilde{\mathbf{m}} = 0$. In order to have objective measures for the stress rate and couple-stress rate, the time derivative given by Green and Naghdi [48] is adopted, *i.e.*,

$$\mathring{\mathbf{T}} = \dot{\mathbf{T}} - \boldsymbol{\Omega}\,\mathbf{T} + \mathbf{T}\,\boldsymbol{\Omega}, \tag{3.5}$$

$$\mathring{\mathbf{M}} = \dot{\mathbf{M}} - \boldsymbol{\Omega}\,\mathbf{M} + \mathbf{M}\,\boldsymbol{\Omega}. \tag{3.6}$$

Herein the angular velocity tensor $\boldsymbol{\Omega}$ is related to the rotation tensor $\mathbf{R}$ and to the rate of rotation tensor, $\dot{\mathbf{R}}$, as $\boldsymbol{\Omega} = \dot{\mathbf{R}}\,\mathbf{R}^T$. In the present paper the following evolution equations for the stress tensor and couple-stress tensor are considered:

$$\mathring{\mathbf{T}} = f_c\,\operatorname{tr}\mathbf{T}\Big[\,\hat{a}^2\,(\mathbf{D}^c + \frac{c}{3}\,(\mathbf{I} : \mathbf{D}^c)\,\mathbf{I}) + (\hat{\mathbf{T}} : \mathbf{D}^c)\,\hat{\mathbf{T}} + \hat{a}\,(\hat{\mathbf{T}} + \hat{\mathbf{T}}^*)\,\|\mathbf{D}^c\|\,\Big], \tag{3.7}$$

$$\mathring{\mathbf{M}} = d_{50}\,f_c\,\operatorname{tr}\mathbf{T}\Big[\,a_m^2\bar{\mathbf{K}} + (\hat{\mathbf{M}} : \bar{\mathbf{K}})\,\hat{\mathbf{M}} + 2\,a_m\,\hat{\mathbf{M}}\,\|\bar{\mathbf{K}}\|\,\Big]. \tag{3.8}$$

Herein $\hat{\mathbf{T}} = \mathbf{T}/\operatorname{tr}\mathbf{T}$, $\hat{\mathbf{T}}^* = \hat{\mathbf{T}} - \mathbf{I}/3$, $\hat{\mathbf{M}} = \mathbf{M}/(d_{50}\operatorname{tr}\mathbf{T})$, $\bar{\mathbf{K}} = d_{50}\mathbf{K}$ are normalized quantities with $\operatorname{tr}\mathbf{T} = \mathbf{I} : \mathbf{T}$ and f_c, $\hat{a}$, c, a_m and d_{50} are scalar factors. The mean grain diameter d_{50} enters the constitutive equations as the internal length. In contrast to earlier micro-polar hypoplastic models a certain simplification is assumed in the present constitutive relations (3.7) and (3.8). In particular, the non-symmetric stress rate is homogeneous of first order in the rate of deformation only and the couple-stress rate is homogeneous of first order in the

rate of curvature only, which is not assumed in the more sophisticated micro-polar hypoplastic models discussed for instance by Tejchman and Gudehus [30], Huang *et al.* [31]. As outlined by Bauer [20] and Gudehus [19], factor f_c with the dimension of stress is usually related to the pressure and density-dependent stiffness under isotropic compression. Here a specific representation of f_c will not be discussed in more detail as it is not relevant to the investigations outlined in Section 5. While in earlier hypoplastic versions the transverse-strain sensitivity of the material was a pure prediction of the constitutive model, a new constant c allows a scaling of the influence of the volume strain rate $\mathbf{I}:\mathbf{D}^c$, which is included as an additional term in the constitutive equation (3.7). It can be concluded from Equation (3.7) that the constant c has no influence for isochoric deformations. In particular for critical states, which are defined for monotonic isochoric deformations without changes of the stress and couple stress state, *i.e.*, $\mathbf{I}:\mathbf{D}^c=0$, $\mathring{\mathbf{T}}=\mathbf{0}$ and $\mathring{\mathbf{M}}=\mathbf{0}$, the constitutive relations (3.7) and Equation (3.8) yield: $\|\hat{\mathbf{T}}^*\|=\hat{a}$ and $\|\hat{\mathbf{M}}\|=a_m$. Thus, the factor $\hat{a}$ is related to the stress limit condition, and factor a_m is related to the couple-stress limit condition in critical states. Factors $\hat{a}$ and a_m reflect the intergranular slide resistance and rotation resistance of particles, respectively [49]. However, for stress states which deviate from critical states, the quantity $\hat{a}$ is not only related to $\|\hat{\mathbf{T}}^*\|$ because the requirement $\hat{a}>0$ must be also fulfilled for isotropic stress states. A consistent adaptation of $\hat{a}$ to the stress limit condition by Matsuoka and Nakai [50] was, for instance, shown by Bauer [51] for a non-polar continuum, which yields for critical states under plane strain conditions:

$$\hat{a}=\sqrt{\frac{8\,\sin^2\varphi_c}{9\,(3+\sin^2\varphi_c)}},$$

and for isotropic stress states:

$$\hat{a}=\sqrt{\frac{8}{3}}\left(\frac{\sin\varphi_c}{3-\sin\varphi_c}\right),$$

Herein φ_c denotes the intergranular friction angle defined for the critical state under triaxial compression. In contrast to a non-polar continuum the stress tensor in a micro-polar continuum is usually non-symmetric, which may lead to a different representation of $\hat{a}$ [37]. For the sake of simplicity $\hat{a}$ and a_m are assumed to be constant in the present paper.

Based on the simplified micro-polar hypoplastic model, an analytical solution for the initial response of plane shearing can be derived for the full set of state quantities involved as outlined in Section 5. In this context it can be noted that the solution for the macro- and micro-spins, the rate of shear stresses and rate of the couple stresses is the same for the simplified micro-polar hypoplastic model and the models proposed by Tejchman and Gudehus [30], Huang *et al.* [31]. However, a different response is obtained for the rate of the normal stresses and the volume strain rate. The analytical solution is restricted to the initial response at the beginning of shearing. For larger shearing the underlying set of differential equations can only be solved numerically and the results are no longer the same for different models.

4. Modeling of plane shearing with dilatancy

For plane shearing of an infinite layer the field quantities are independent of the co-ordinate in the direction of shearing, *i.e.*, $\partial(.)/\partial x_1=0$ with respect to the co-ordinate system shown in Figure 1. For plane-strain conditions the field quantities are also independent of the co-ordinate x_3. Then the macro-motion can be described by $x_1=X_1+f_1(X_2,t)$, $x_2=X_2+f_2(X_2,t)$ and $x_3=X_3$, where the spatial co-ordinates x_i $(i=1,2,3)$ represent the current position of a

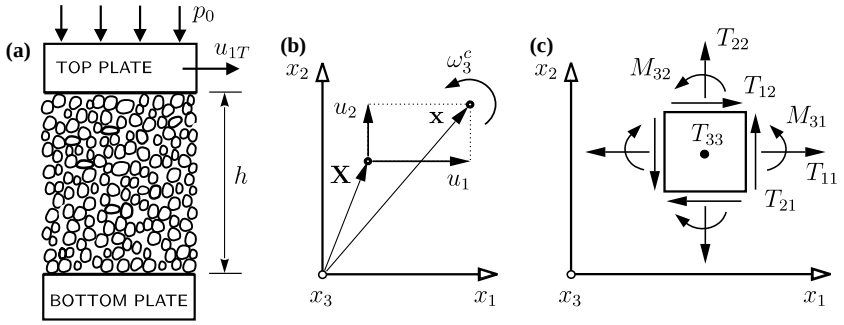

Figure 1. Modeling of plane shearing under constant vertical pressure $p_0 = -\sigma_{22}$: (a) section of the infinite granular layer between parallel plates with rough surfaces, (b) kinematics of plane shearing with dilatancy and degrees of freedom u_1, u_2 and ω_3, (c) stress components σ_{11}, σ_{22}, σ_{33}, σ_{12}, σ_{21} and couple-stress components M_{31} and M_{32} with respect to the Cartesian co-ordinate system.

particle and X_i $(i=1,2,3)$ are the corresponding co-ordinates in the initial configuration. The functions $f_i(X_2,t)$ $(i=1,2)$ are time-dependent functions with respect to $f_i(X_2,t=0)=0$ in the initial configuration at time $t=0$. The only possible micro-motion is the micro-rotation or so-called Cosserat rotation ω_3^c which is orientated perpendicular to the (x_1,x_2) plane as shown in Figure 1. The displacements $u_i = x_i - X_i$ read: $u_1 = f_1(X_2,t)$, $u_2 = f_2(X_2,t)$ and $u_3 = 0$. Since u_2 depends on X_2, the kinematics of shearing with dilatancy is taken into account. With respect to

$$g_i(X_2,t) = \frac{\partial f_i(X_2,t)}{\partial X_2} \quad \text{and} \quad \dot{g}_i(X_2,t) = \frac{d\, g_i(X_2,t)}{d\, t} \quad (i=1,2), \tag{4.1}$$

for any field variable ϕ defined in the infinite layer, the following relations are valid:

$$\frac{\partial \phi}{\partial X_1} = \frac{\partial \phi}{\partial x_1} = 0, \qquad \frac{\partial \phi}{\partial X_2} = (1+g_2)\,\frac{\partial \phi}{\partial x_2}, \qquad \frac{\partial \phi}{\partial X_3} = \frac{\partial \phi}{\partial x_3} = 0. \tag{4.2}$$

Therefore the non-vanishing components of the velocity gradient and macro-spin read:

$$L_{12} = \frac{\partial \dot{u}_1}{\partial x_2} = \frac{\dot{g}_1}{1+g_2}, \qquad L_{22} = \frac{\partial \dot{u}_2}{\partial x_2} = \frac{\dot{g}_2}{1+g_2}, \qquad W_{12} = \frac{1}{2}\,\frac{\partial \dot{u}_1}{\partial x_2} = -\dot{\omega}_3. \tag{4.3}$$

It follows from L_{22} in (4.3) that $\dot{g}_2/(1+g_2)$ is equal to the volume strain rate and therefore a measure of the dilatancy behavior of the granular layer. As body forces, body couples and inertia forces are neglected, the equilibrium equations (3.3) and (3.4) reduce to:

$$\frac{\partial T_{ij}}{\partial x_j} = 0, \qquad \frac{\partial M_{ij}}{\partial x_j} - \epsilon_{ikl}\, T_{kl} = 0. \tag{4.4}$$

With respect to the relations in (4.2) the time derivative of Equations (4.4) reads:

$$\frac{\partial \dot{T}_{ij}}{\partial x_j} - \frac{\partial T_{ij}}{\partial x_m}\,\frac{\partial \dot{u}_m}{\partial x_j} = 0, \tag{4.5}$$

and

$$\frac{\partial \dot{M}_{ij}}{\partial x_j} - \frac{\partial M_{ij}}{\partial x_m}\,\frac{\partial \dot{u}_m}{\partial x_j} - \epsilon_{ikl}\, \dot{T}_{kl} = 0. \tag{4.6}$$

For the infinite sheared layer Equations (4.5) and (4.6) yield:

$$\frac{\partial \dot{T}_{12}}{\partial x_2} = 0, \qquad \frac{\partial \dot{T}_{22}}{\partial x_2} = 0, \tag{4.7}$$

$$\frac{\partial \dot{M}_{32}}{\partial x_2} - \frac{\dot{g}_2}{1+g_2}(T_{12} - T_{21}) - (\dot{T}_{12} - \dot{T}_{21}) = 0. \tag{4.8}$$

The material derivatives $\dot{T}_{ij}$ and $\dot{M}_{ij}$ in (4.7) and (4.8) are related to the constitutive equations using the corresponding objective derivatives defined in (3.5) and (3.6). For plane shearing the components of the objective stress rate and couple stress rate read:

$$\begin{aligned}
\mathring{T}_{11} &= f_c \left[\hat{a}^2 \, (c/3) \, D^c_{22} + \psi_1 \, \hat{T}_{11} + \hat{a} \, (2\,\hat{T}_{11} - 1/3) \sqrt{\psi_2} \right], \\
\mathring{T}_{22} &= f_c \left[\hat{a}^2 \, (D^c_{22} + (c/3) \, D^c_{22}) + \psi_1 \, \hat{T}_{22} + \hat{a} \, (2\,\hat{T}_{22} - 1/3) \sqrt{\psi_2} \right], \\
\mathring{T}_{33} &= f_c \left[\hat{a}^2 \, (c/3) \, D^c_{22} + \psi_1 \, \hat{T}_{33} + \hat{a} \, (2\,\hat{T}_{33} - 1/3) \sqrt{\psi_2} \right], \\
\mathring{T}_{12} &= f_c \left[\hat{a}^2 \, D^c_{12} + \left(\psi_1 + 2\,\hat{a} \sqrt{\psi_2} \right) \hat{T}_{12} \right], \\
\mathring{T}_{21} &= f_c \left[\hat{a}^2 \, D^c_{21} + \left(\psi_1 + 2\,\hat{a} \sqrt{\psi_2} \right) \hat{T}_{21} \right], \\
\mathring{M}_{31} &= d_{50} \, f_c \left[\left(\hat{M}_{32} \, \bar{K}_{32} + 2\,a_m \sqrt{\bar{K}^2_{32}} \right) \hat{M}_{31} \right], \\
\mathring{M}_{32} &= d_{50} \, f_c \left[a^2_m \, \bar{K}_{32} + \left(\hat{M}_{32} \, \bar{K}_{32} + 2\,a_m \sqrt{\bar{K}^2_{32}} \right) \hat{M}_{32} \right],
\end{aligned} \tag{4.9}$$

with the abbreviations.

$$\psi_1 = \hat{T}_{12} \, D^c_{12} + \hat{T}_{21} \, D^c_{21} + \hat{T}_{22} \, D^c_{22}, \qquad \psi_2 = D^{c\,2}_{12} + D^{c\,2}_{21} + D^{c\,2}_{22},$$

and the kinematic quantities

$$D^c_{12} = \dot{\omega}^c_3 + \frac{\dot{g}_1}{1+g_2}, \qquad D^c_{21} = -\dot{\omega}^c_3, \qquad D^c_{22} = \frac{\dot{g}_2}{1+g_2}, \qquad \bar{K}_{32} = d_{50} \, \frac{\partial \dot{\omega}^c_3}{\partial x_2}.$$

While the symmetry condition for the infinite shear layer was already considered above, the boundary conditions at the bottom and top of the layer are still to be specified. Apart from the displacement and stress boundary conditions of the classical continuum, micro-rotation and couple-stress boundary conditions occur in a micro-polar continuum. Herein the micro-polar boundary conditions allow the modeling of the influence of the rotation resistance of particles in contact with a rough bounding structure, as has been discussed in more detail, for instance by Tejchman [28] and Bauer and Huang [34]. For the present investigation the bottom of the layer is assumed to be fixed so that neither sliding nor rotation may occur, *i.e.*,

$$x_2 = 0: \qquad \dot{u}_1 = 0, \qquad \dot{u}_2 = 0, \qquad \dot{\omega}^c_3 = 0. \tag{4.10}$$

At the top of the layer a vertical pressure is applied and kept constant, *i.e.*, $\dot{T}_{22}=0$. The horizontal velocity $\dot{u}_{1T}$ and the rate of the micro-rotation $\dot{\omega}^c_{3T}$ are prescribed, *i.e.*,

$$x_2=h: \quad \dot{u}_1=\dot{u}_{1T}, \qquad \dot{\omega}^c_3=\dot{\omega}^c_{3T}, \qquad \dot{T}_{22}=0\,. \tag{4.11}$$

5. Analytical solution for the initial response

For the investigation of the initial response of an infinite sheared layer the following homogeneous and initially isotropic state is considered:

$$T_{ij}=-p_0\,\delta_{ij}, \qquad M_{ij}=0, \tag{5.1}$$

where p_0 denotes the isotropic initial pressure. It follows from the relations in (5.1) that in the initial state the shear stresses and couple stresses are assumed to be zero; thus, the material time derivatives of the stresses and the couple stresses coincide with the objective rates at the beginning of shearing. When this property is taken into account and with respect to $g_1=g_2=0$ and the initial state assumed in (5.1), the relations for the non-zero rate of the stress and couple-stress components by (4.9) reduce to:

$$\dot{T}_{11}=\mathring{\dot{T}}_{11}=f_c\left[\hat{a}^2\,\frac{c}{3}\,\dot{g}_2+\frac{\dot{g}_2}{9}+\frac{\hat{a}}{3}\sqrt{\dot{g}_2^2+(\dot{\omega}^c_3+\dot{g}_1)^2+\dot{\omega}^{c\,2}_3}\right], \tag{5.2}$$

$$\dot{T}_{22}=\mathring{\dot{T}}_{22}=f_c\left[\hat{a}^2\left(1+\frac{c}{3}\right)\dot{g}_2+\frac{\dot{g}_2}{9}+\frac{\hat{a}}{3}\sqrt{\dot{g}_2^2+(\dot{\omega}^c_3+\dot{g}_1)^2+\dot{\omega}^{c\,2}_3}\right], \tag{5.3}$$

$$\dot{T}_{33}=\mathring{\dot{T}}_{33}=\dot{T}_{11}, \tag{5.4}$$

$$\dot{T}_{12}=\mathring{\dot{T}}_{12}=f_c\,\hat{a}^2\,(\dot{\omega}^c_3+\dot{g}_1), \tag{5.5}$$

$$\dot{T}_{21}=\mathring{\dot{T}}_{21}=-f_c\,\hat{a}^2\,\dot{\omega}^c_3, \tag{5.6}$$

$$\dot{M}_{32}=\mathring{\dot{M}}_{32}=f_c\,a_m^2\,d_{50}^2\,K_{32}. \tag{5.7}$$

Herein the quantities:

$$\dot{g}_1=\frac{\mathrm{d}\dot{u}_1}{\mathrm{d}x_2}=-2\,\dot{\omega}_3, \qquad \dot{g}_2=\frac{\mathrm{d}\dot{u}_2}{\mathrm{d}x_2}, \qquad \dot{\omega}^c_3 \quad \text{and} \quad K_{32}=\frac{\mathrm{d}\dot{\omega}^c_3}{\mathrm{d}x_2} \tag{5.8}$$

have to be determined for the given boundary value problem as outlined in the following section.

5.1. General solution

With respect to the requirement in (4.7) the quantity $\dot{T}_{12}$ in (5.5) is constant across the height of the layer, *i.e.*,

$$\dot{T}_{12}=f_c\,\hat{a}^2\,(\dot{\omega}^c_3+\dot{g}_1)=\chi\,, \tag{5.9}$$

where χ denotes a constant. By substituting the relations (5.5–5.7) in (4.8), one obtains

$$\frac{\partial}{\partial x_2}\left(f_c\,a_m^2\,d_{50}^2\,\frac{\partial\dot{\omega}^c_3}{\partial x_2}\right)-f_c\,\hat{a}^2\,(2\,\dot{\omega}^c_3+\dot{g}_1)=0. \tag{5.10}$$

For an initially homogeneous layer, f_c, $\hat{a}$ and d_{50} are independent of the co-ordinates x_i ($i = 1, 2, 3$) so that (5.10) and (5.9) lead to the following differential equation for $\dot{\omega}_3^c$

$$\eta^2 \frac{\mathrm{d}^2 \dot{\omega}_3^c}{\mathrm{d}x_2^2} - \dot{\omega}_3^c = C_1, \tag{5.11}$$

with the abbreviations

$$\eta = \frac{a_m}{\hat{a}} d_{50} \quad \text{and} \quad C_1 = \frac{\chi}{f_c \hat{a}^2} = \dot{\omega}_3^c + \dot{g}_1.$$

The general solution to the second-order differential equation (5.11) reads

$$\dot{\omega}_3^c = C_2 \cosh(x_2/\eta) + C_3 \sinh(x_2/\eta) - C_1, \tag{5.12}$$

where C_2 and C_3 are integration constants. The derivative of $\dot{\omega}_3^c$ yields the rate of curvature, *i.e.*,

$$K_{32} = \frac{\mathrm{d}\dot{\omega}_3^c}{\mathrm{d}x_2} = \frac{1}{\eta} \left[C_2 \sinh(x_2/\eta) + C_3 \cosh(x_2/\eta) \right]. \tag{5.13}$$

Inserting $\dot{g}_1 = -2\,\dot{\omega}_3$ in (5.9), one obtains for the rate of the macro-spin

$$\dot{\omega}_3 = \frac{1}{2} \left[\dot{\omega}_3^c - C_1 \right] = \frac{1}{2} \left[C_2 \cosh(x_2/\eta) + C_3 \sinh(x_2/\eta) \right] - C_1, \tag{5.14}$$

and for the quantity $\dot{g}_1$

$$\dot{g}_1 = -2\,\dot{\omega}_3 = 2\,C_1 - \left[C_2 \cosh(x_2/\eta) + C_3 \sinh(x_2/\eta) \right]. \tag{5.15}$$

With respect to (5.8) the integration of $\mathrm{d}\dot{u}_1 = -2\,\dot{\omega}_3\,\mathrm{d}x_2$ yields the initial rate of the horizontal displacement u_1 as a function of the co-ordinate x_2, *i.e.*,

$$\dot{u}_1 = 2\,C_1\,x_2 - C_2\,\eta \sinh(x_2/\eta) - C_3\,\eta \cosh(x_2/\eta) + C_4. \tag{5.16}$$

Taking into account a constant vertical pressure applied at the top of the layer, and the requirement for equilibrium across the height of the layer, one observes that $\dot{T}_{22}$ is zero within the shear layer. Inserting $\dot{T}_{22} = 0$ and $\dot{\omega}_3^c$ from (5.12) in (5.3) yields an equation for $\dot{g}_2$ with the solution

$$\dot{g}_2 = -\sqrt{\frac{C_1^2 + [C_2 \cosh(x_2/\eta) + C_3 \sinh(x_2/\eta) - C_1]^2}{[\hat{a}(3+c) + 1/(3\,\hat{a})]^2 - 1}}. \tag{5.17}$$

The initial rate of the vertical displacement u_2 can be obtained by integration of $\mathrm{d}\dot{u}_2 = \dot{g}_2\,\mathrm{d}x_2$, *i.e.*,

$$\dot{u}_2 = -\int \sqrt{\frac{C_1^2 + [C_2 \cosh(x_2/\eta) + C_3 \sinh(x_2/\eta) - C_1]^2}{[\hat{a}(3+c) + 1/(3\,\hat{a})]^2 - 1}}\,\mathrm{d}x_2 + C_5. \tag{5.18}$$

By inserting $\dot{\omega}_3^c$, K_{32}, $\dot{g}_1$ and $\dot{g}_2$ into (5.2) to (5.7), one obtains the following relations for the initial rate of the normalized quantities of the stress and couple stress components

$$\frac{\dot{T}_{11}}{f_c\,\hat{a}^2} = \left[\frac{c}{3} - \frac{1}{9\,\hat{a}^2}\right]\left[\frac{C_1^2 + [C_2\,\cosh(x_2/\eta) + C_3\,\sinh(x_2/\eta) - C_1]^2}{[\hat{a}(3+c) + 1/(3\,\hat{a})]^2 - 1}\right] + \\ + \frac{1}{3\,\hat{a}}\left[\frac{C_1^2 + [C_2\,\cosh(x_2/\eta) + C_3\,\sinh(x_2/\eta) - C_1]^2}{1 - 1/[\hat{a}(3+c) + 1/(3\,\hat{a})]^2}\right]^{1/2}, \tag{5.19}$$

$$\frac{\dot{T}_{33}}{f_c\,\hat{a}^2} = \frac{\dot{T}_{11}}{f_c\,\hat{a}^2}, \qquad \frac{\dot{T}_{12}}{f_c\,\hat{a}^2} = C_1, \tag{5.20}$$

$$\frac{\dot{T}_{21}}{f_c\,\hat{a}^2} = -\,C_2\,\cosh(x_2/\eta) - C_3\,\sinh(x_2/\eta) + C_1, \tag{5.21}$$

$$\frac{\dot{M}_{32}}{f_c\,\hat{a}\,a_m\,d_{50}} = C_2\,\sinh(x_2/\eta) + C_3\,\cosh(x_2/\eta) \tag{5.22}$$

with $\eta = (a_m/\hat{a})d_{50}$. The general solution shows that, even for the case of an initially isotropic stress state and zero couple stresses, the initial rate of the state quantities under shearing is different from the classical non-polar continuum in the case of non-vanishing constants C_2 and C_3. With the exception of $\dot{T}_{12}$ the rates of the state quantities are nonlinear functions of the co-ordinate x_2 as a result of the micro-polar quantities contained in the present micro-polar hypoplastic model. Furthermore, it follows from relation (5.17) that a transverse-strain sensitivity, which is controlled by the constitutive constant c, influences the volume strain rate $\mathbf{I}:\mathbf{D}^c = \dot{g}_2$, and consequently also the velocity $\dot{u}_2$ and the stress rates $\dot{T}_{11}$ and $\dot{T}_{33}$. It can also be noted that, for real solutions for $\dot{g}_2$, the denominator of the expression (5.17) must be greater than zero, which yields a lower bound for the calibration of the value of c.

Across the height of the sheared layer the distribution of the quantities (5.12) to (5.22) is strongly influenced by the interface behavior between the granular layer and the rough bounding plates. The interface behavior can be taken into account by specifying the constants C_i $(i = 1{\cdot}5)$ as outlined in the next section.

5.2. Influence of the micro-polar boundary conditions

The boundary conditions at the bottom and top surfaces specified in (4.10) and (4.11) yield for the constants C_i $(i = 1{\cdot}5)$:

$$C_1 = \frac{\dot{u}_{1T}/\eta + \dot{\omega}_{3T}^c\,\tanh(h/(2\,\eta))}{2\,[h/\eta - \tanh(h/(2\,\eta))]}, \qquad C_2 = C_1, \tag{5.23}$$

$$C_3 = \frac{\dot{\omega}_{3T}^c\,[(2\,h/\eta)/\sinh(h/\eta) - 1] - (\dot{u}_{1T}/\eta)\,\tanh(h/(2\,\eta))}{2\,[h/\eta - \tanh(h/(2\,\eta))]}, \tag{5.24}$$

$$C_4 = \eta\,C_3, \quad C_5 = \left[\int \dot{g}_2\,\mathrm{d}x_2\right]_{x_2=0}, \quad \text{with: } \eta = \frac{a_m}{\hat{a}}d_{50}. \tag{5.25}$$

In the following the influence of the micro-polar boundary conditions on the initial response will be discussed for a shear layer with a height of $h = 1\,\mathrm{cm}$, a prescribed horizontal shear velocity of $\dot{u}_{1T} = 1\,\mathrm{cm/s}$, a constant vertical pressure and the constitutive constants: $d_{50} = 0{\cdot}05$ cm, $\hat{a} = 0{\cdot}33$, $a_m = 1$ and $c = 0$ which are relevant for a medium quartz sand with a critical friction angle of $\varphi_c = 30^\circ$. For the present discussion the value of the constant f_c is not relevant as the rates of the stress- and couple stress components can be normalized by f_c.

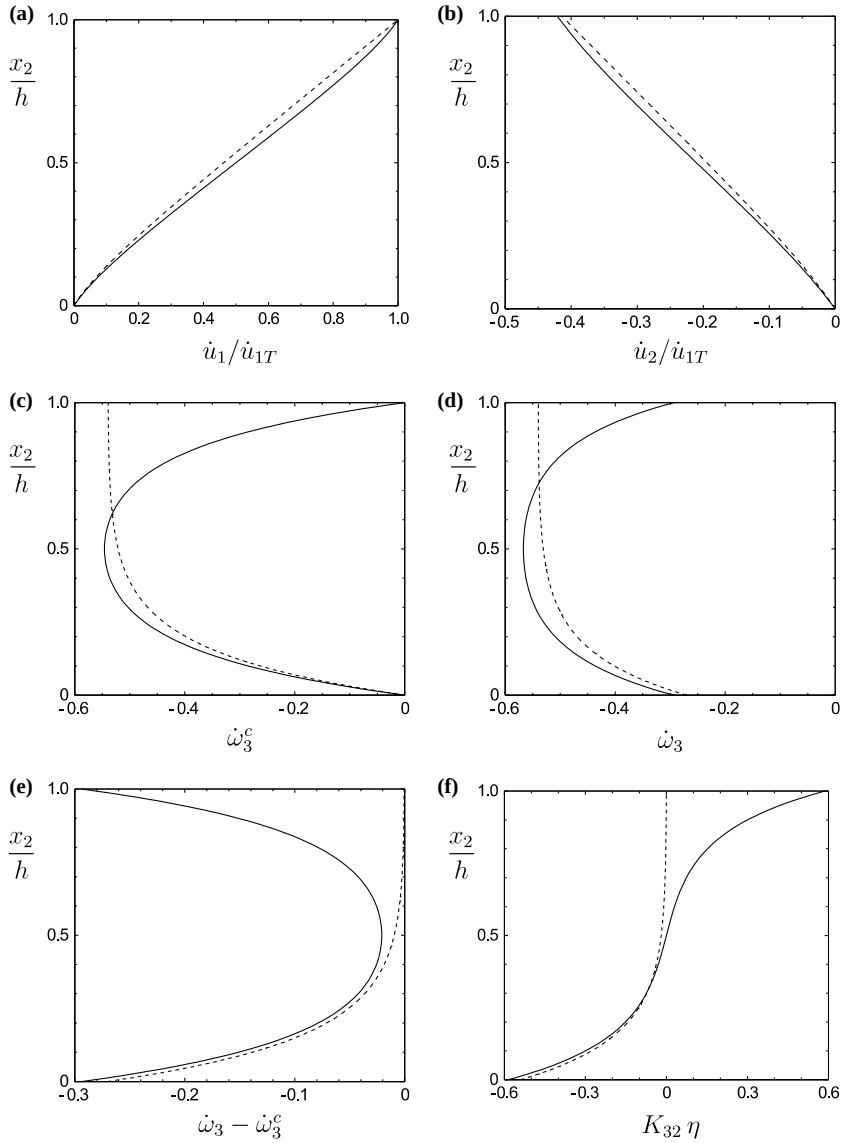

Figure 2. Initial response of a sheared layer for the boundary conditions at the bottom $x_2 = 0 : \dot{u}_1 = \dot{u}_2 = 0$, $\dot{\omega}_{3B}^c = 0$, and at the top $x_2 = h : \dot{u}_1 = \dot{u}_{1T}$, $\dot{T}_{22} = 0$, $\dot{\omega}_{3T}^c = 0$ (solid curve) and $\dot{M}_{32T} = 0$ (dotted curve). Distribution of: (a) horizontal velocity $\dot{u}_1$, (b) vertical velocity $\dot{u}_2$, (c) micro-rotation rate $\dot{\omega}_3^c$, (d) macro-rotation rate $\dot{\omega}_3$, (e) difference of macro- and micro-rotation rates $\dot{\omega}_3 - \dot{\omega}_3^c$, and (f) curvature rate K_{32}.

Figures (2) and (3) show the initial response of the shear layer for two different micro-polar boundary conditions prescribed at the top surface. The solid curves show the results obtained for $\dot{\omega}_3^c(x_2 = h) = \dot{\omega}_{3T}^c = 0$ and the dotted curves are obtained for the assumption of a zero couple stress rate $\dot{M}_{32}(x_2 = h) = \dot{M}_{32T} = 0$.

The special case $\dot{\omega}_{3T}^c = 0$ reflects the behavior of a very rough top surface without particle rotation along the interfaces. The same assumption was introduced in (4.10) for the bottom surface, so that the micro-polar boundary conditions are symmetric for this case. Figure 2a and 2b shows that the velocities $\dot{u}_1(x_2)$ and $\dot{u}_2(x_2)$ are nonlinearly distributed across the height of the shear layer. Thus, in a micro-polar continuum the deformation is inhomogeneous from the beginning of shearing. The distribution of the rate of micro-rotation

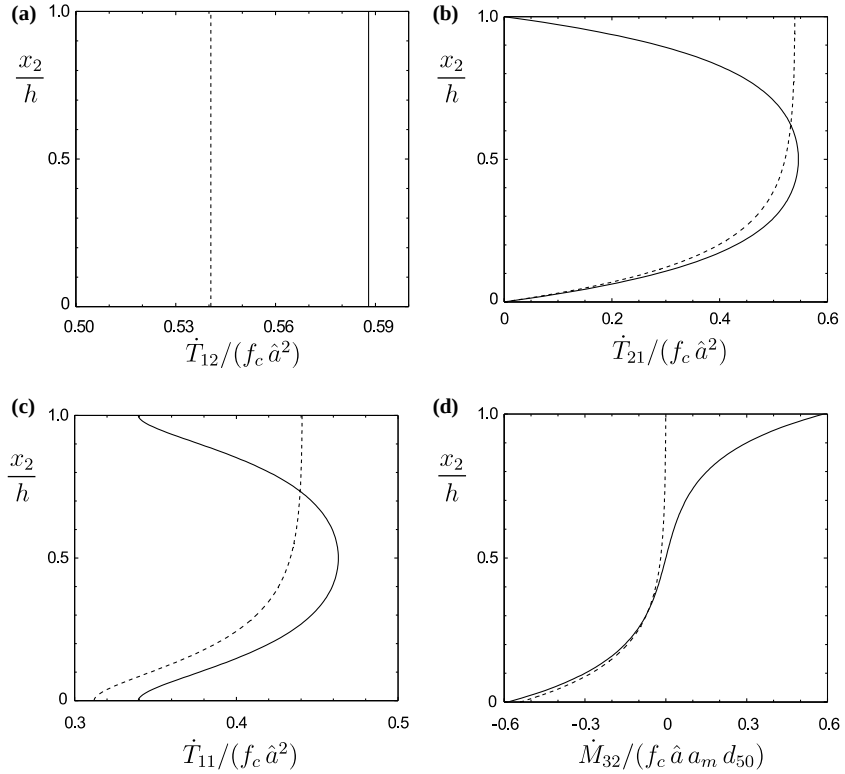

Figure 3. Initial response of a sheared layer for the boundary conditions at the bottom $x_2=0:\dot{u}_1=\dot{u}_2=0$, $\dot{\omega}^c_{3B}=0$, and at the top $x_2=h:\dot{u}_1=\dot{u}_{1T}$, $\dot{T}_{22}=0$, $\dot{\omega}^c_{3T}=0$ (solid curve) and $\dot{M}_{32T}=0$ (dotted curve). Distribution of the normalized: (a) shear stress rate $\dot{T}_{12}$, (b) shear-stress rate $\dot{T}_{21}$, (c) normal-stress rate $\dot{T}_{11}=\dot{T}_{33}$, and (d) couple-stress rate $\dot{M}_{32}$.

(Figure 2c) and the rate of macro-rotation (Figure 2d) are also nonlinear and they are different from each other (Figure 2e). With respect to the rule of signs in Figure 1a negative micro-rotation rate means clockwise rotation for a movement of the top surface to the right. The extreme values of $\dot{\omega}^c_3$ and of $\dot{\omega}_3$ occur in the middle of the layer. The gradient of the micro-rotation is termed rate of curvature, K_{32}, and shown in Figure 2f. From Figure 2e it can be concluded that, at the beginning of shearing, the influence of micro-polar properties is more pronounced close to the bottom and top boundaries of the layer. The shear-stress rate $\dot{T}_{12}$ is constant as is necessary for equilibrium (Figure 3a) and it is different from the shear stress rate $\dot{T}_{21}$ (Figure 3b). Therefore, the stress tensor also becomes non-symmetric in the case of an initially isotropic stress state. The distribution of the normal stress rate $\dot{T}_{11}$ is nonlinear (Figure 3c) and it is equal to the normal stress rate $\dot{T}_{33}$. The normalized quantity of the couple-stress rate $\dot{M}_{32}$ (Figure 3d) coincides with the normalized curvature rate K_{32} shown in Figure 2f which is due to relation (5.7). Although the couple-stress rate is zero in the middle of the layer for symmetric micro-polar boundary conditions, *i.e.*, $\dot{M}_{32}(x_2=h/2)=0$, the shear stress rate $\dot{T}_{12}(x_2=h/2)$ is different from the shear-stress rate $\dot{T}_{21}(x_2=h/2)$. Thus, $\partial\dot{M}_{32}/\partial x_2\neq 0$ holds for $x_2=h/2$ and depends on the height h of the shear layer according to

$$\left[\frac{\partial\dot{M}_{32}}{\partial x_2}\right]_{x_2=h/2}=\frac{f_c\,\hat{a}^2\,\dot{u}_1/(h/\eta)}{2[(h/\eta)\,\cosh(h/(2\eta))-\sinh(h/(2\eta))]}. \tag{5.26}$$

The results indicate that micro-polar effects appear across the entire height of the shear layer and a localization of the deformation is not manifested at the beginning of shearing.

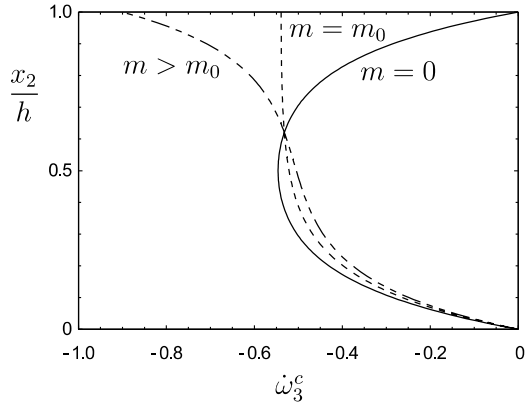

Figure 4. Distribution of initial rate of the micro-polar rotation, $\dot{\omega}_3^c$, for the boundary conditions at the bottom $x_2 = 0 : \dot{u}_1 = \dot{u}_2 = 0$, $\dot{\omega}_{3B}^c = 0$, and at the top $x_2 = h : \dot{u}_1 = \dot{u}_{1T}$, $\dot{T}_{22} = 0$, $m = 0$ (solid curve), $m = m_0$ (dotted curve) and $m > m_0$ (chain-dotted curve).

Numerical simulations of large shearing show that shear localization takes place with advanced shearing in the area of the maximum magnitude of the rate of the micro-rotations; see *e.g.* [38, pp. 79–85], [30,49,52]. Thus, the extreme value of the rate of micro-rotations obtained for the initial response (Figure 2c) is an indicator of where shear-strain localization may develop under continuous shearing.

Another case of interest arises for a zero couple-stress rate along the top surface. The boundary condition $\dot{M}_{32}(x_2 = h) = \dot{M}_{32T} = 0$ can alternatively be expressed by the corresponding micro-rotation:

$$\dot{\omega}_3^c(x_2 = h) = \dot{\omega}_{3T}^c = -m_0 \frac{\dot{u}_{1T}}{\eta}, \tag{5.27}$$

with:

$$m_0 = \frac{1 - 1/\cosh(h/\eta)}{2[h/\eta - \tanh(h/\eta)]}, \quad \eta = \frac{a_m}{\hat{a}} d_{50}.$$

Together with $\dot{\omega}_{3B}^c = 0$ prescribed at the bottom of the layer the micro-polar boundary conditions are no longer symmetric. By inserting relation (5.27) for $\dot{\omega}_{3T}^c$ in (5.23–5.25), one obtains the initial response of the shear layer for the boundary conditions $\dot{\omega}_{3B}^c = 0$ and $\dot{M}_{32T} = 0$ (dotted curves in Figure 2 and Figure 3). At the beginning of shearing the distribution of the velocities $\dot{u}_1(x_2)$ (Figure 2a) and $\dot{u}_2(x_2)$ (Figure 2b) is again nonlinear and almost the same as for the case of $\dot{\omega}_{3T}^c = 0$. The further evolution of these quantities, however, can be quite different when shear localization appears under larger shearing, as can be shown by numerical simulations; see *e.g.* [49]. In contrast with the results obtained for the boundary condition $\dot{\omega}_{3T}^c = 0$, the extreme value of the micro-rotation (Figure 2c) and macro-rotation (Figure 2d) occurs at the top of layer. Both $\mathrm{d}\dot{\omega}_3/\mathrm{d}x_2$ and $\mathrm{d}\dot{\omega}_3^c/\mathrm{d}x_2$ are zero at the top of the layer, which underlines the meaning of $\dot{M}_{32T} = 0$ as a special boundary condition, where the curvature rate $K_{32} = \mathrm{d}\dot{\omega}_3^c/\mathrm{d}x_2$ changes sign (Figure 4). The normalized quantity of the couple-stress rate $\dot{M}_{32}$ (Figure 3d) again coincides with the curvature rate K_{32} and the initial shear-stress rate $\dot{T}_{12}$ (Figure 3a) is a little lower than for the symmetric boundary conditions, $\dot{\omega}_{3B}^c = \dot{\omega}_{3T}^c = 0$. In contrast with the results obtained for symmetric boundary conditions, the maximum shear stress rate $\dot{T}_{21}$ (Figure 3b) and the maximum normal-stress rates $\dot{T}_{11} = \dot{T}_{33}$ (Figure 3c) occur at the top of the layer when a zero couple-stress rate is prescribed.

It follows from relation (5.27) that, for $\dot{M}_{32T}=0$, the micro-rotation rate $\dot{\omega}^c_{3T}$ along the top boundary is proportional to the prescribed horizontal shear displacement $\dot{u}_{1T}$. The evolution of the state quantities are also determined by the height of the shear layer because the factor m_0 depends on h. By replacing m_0 with an arbitrary factor m relation (5.27) agrees with the empirical formula proposed by Tejchman [28] to model the influence of a rough bounding surface on the rotation resistance of particle in contact with the bounding structure. Numerical simulations by Huang *et al.* [52] show that the location and thickness of shear-strain localization is strongly influenced by the value of the factor m. In particular for $m=0$ the case of a very rough top surface without particle rotations is modeled which shows an extreme value of micro-rotations in the middle of the shear layer. For $0<m<m_0$ the extreme value of micro-rotations and consequently the location where shear-strain localization takes place is located within the upper part of the shear layer. For $m>m_0$ shear-strain localization takes place very close to the top boundary and the thickness of the localized zone is smaller than for $m<m_0$. The influence of m on the initial response of the micro-rotations is demonstrated in Figure 4 for different values for m. It is obvious that m determines the sign of the curvature rate $K_{32}=\mathrm{d}\dot{\omega}^c_3/\mathrm{d}x_2$ and the location of maximum micro-rotation. At the top of the layer the curvature rate is positive for $m<m_0$, negative for $m>m_0$ and zero for $m=m_0$. The latter is related to $\dot{M}_{32T}=0$.

For prescribed zero couple-stress rates along the bottom and top surfaces the response of the shear layer coincides with the results obtained for the classical non-polar continuum. In particular the constants C_2 and C_3 become zero by inserting the boundary conditions $\dot{M}_{32}(x_2=0)=\dot{M}_{32}(x_2=h)=0$ in relation (5.22). Consequently relation (5.16) yields $C_4=0$ for the bottom boundary condition $\dot{u}_1(x_2=0)=0$, and with respect to the prescribed horizontal shear velocity $\dot{u}_1(x_2=h)=\dot{u}_{1T}$ at the top of the layer one obtains $C_1=\dot{u}_{1T}/(2h)$. For the bottom boundary condition $\dot{u}_2(x_2=0)=0$ relation (5.18) yields $C_5=0$. Then the couple stresses are zero, the micro-rotation rate corresponds to the macro-rotation rate, the shear stresses are symmetric and the velocity profile is linear across the height of the layer, *i.e.*,

$$\dot{\omega}^c_3=\dot{\omega}_3=-\dot{u}_{1T}/(2h), \quad K_{32}=0, \tag{5.28}$$

$$\dot{g}_1=\dot{u}_{1T}/h, \quad \dot{u}_1=(\dot{u}_{1T}/h)\,x_2, \tag{5.29}$$

$$\dot{g}_2=-\sqrt{2[\dot{u}_{1T}/(2h)]^2/[[\hat{a}(3+c)+1/(3\hat{a})]^2-1]}, \tag{5.30}$$

$$\dot{u}_2=-\sqrt{2[\dot{u}_{1T}/(2h)]^2/[[\hat{a}(3+c)+1/(3\hat{a})]^2-1]}\,x_2, \tag{5.31}$$

$$\dot{T}_{11}=\dot{T}_{33}=f_c\sqrt{2\hat{a}^2/[[\hat{a}(3+c)+1/(3\hat{a})]^2-1]}\,\dot{u}_{1T}/(2h), \tag{5.32}$$

$$\dot{T}_{12}=\dot{T}_{21}=f_c\hat{a}^2\,\dot{u}_{1T}/(2h), \quad \dot{M}_{32}=0. \tag{5.33}$$

It follows from (5.28) to (5.33) that for the couple-stress boundary conditions $\dot{M}_{32}(x_2=0)=\dot{M}_{32}(x_2=h)=0$ no polar properties appear within the shear layer. Numerical simulations show, however, that for continued shearing the non-polar solution is unstable. Any perturbation immediately leads to the polar solution. This phenomenon was termed "spontaneous polarisation" by Gudehus [53].

6. Conclusion

The influence of particle rotation and couple stresses in granular materials has been modeled with a micro-polar hypoplastic continuum approach. The evolution equations for the non-symmetric stress tensor and the couple-stress tensor are nonlinear isotropic tensor-valued functions, which are homogeneous of first order in the rate of deformation and rate of curvature. For an infinite strip of a micro-polar hypoplastic material located between two parallel plates under plane shearing an analytical solution has been derived. The general solution shows that polar quantities appear within the shear layer from the beginning of shearing. In contrast with the classical non-polar continuum the shear velocity and dilatancy velocity are nonlinearly distributed across the height of the shear layer, even if the material is homogeneous and non-polarized in the initial state. The macro-rotation rate is not constant and differs from the micro-rotation rate. Shear stresses are non-symmetric and the stress and couple-stress rates are distributed nonlinearly. The distribution of the state quantities within the shear layer strongly depends on the prescribed micro-polar boundary conditions which reflect the rotation resistance of the particles against the surface of the bounding structure. This is demonstrated for two different wall boundary conditions at the top of the shear layer. For the interaction with a very rough wall particle rotations are prevented, which can be modeled with locked micro-rotations along this boundary. Then the corresponding couple-stress rate shows an extreme value at this boundary. The results for the rate of the state quantities obtained for zero couple-stress rates prescribed along one of the boundaries show a non-symmetric distribution within the shear layer. The same result as for the non-polar continuum is obtained for the special case of zero couple-stress rates prescribed at both the bottom and the top boundaries. For an initially homogeneous and isotropic state, an analytical solution for the present micro-polar hypoplastic material model under plane shearing is restricted to the initial response. In general, the underlying set of differential equations for continuous shearing can only be solved numerically.

References

1. V.K. Garga and J.A. Infante Sedano, Steady state strength of sands in a constant volume ring shear apparatus. *Geotech. Testing J.* 25 (2002) 414–421.
2. K.H. Roscoe, The influence of strains in soil mechanics, 10th Rankine Lecture. *Géotechnique* 20 (1970) 129–170.
3. H.B. Mühlhaus and I. Vardoulakis, The thickness of shear bands in granular materials. *Geotechnique* 37 (1987) 271–283.
4. M. Oda, Micro-fabric and couple stress in shear bands of granular materials. In: C.C. Thornton (ed.), *Powders and Grains*, 3. Rotterdam: Balkema (1993) pp. 161–167.
5. J. Desrues, R. Chambon, M. Mokni and F. Mazerolle, Void ratio evolution inside shear bands in triaxial sand specimens studied by computed tomography. *Géotechnique* 46 (1996) 529–546
6. E. Cosserat and F. Cosserat, Théorie des Corps Deformables. *Herman et fils*, Paris (1909).
7. R.D. Mindlin, Stress functions for a Cosserat continuum. *Int. J. Solids Struct*. 1 (1965) 265–271.
8. A.C. Eringen, Polar and nonlocal field theories. *Continuum Physics* IV. New York, San Francisco, London: Academic Press (1976) 274 pp.
9. E.C. Aifantis, On the microstructural original of certain inelastic models. *J. Engng. Mat. Technol.* 106 (1984) 326–334.
10. Z.P. Bazant, T.B. Belytschko and T.P. Chang, Continuum theory for strain softening. *ASCE J. Engng. Mech.* 110 (1984) 1666–1692.
11. H.-B. Mühlhaus, Application of Cosserat theory in numerical solutions of limit load problems. *Ingenieur Archiv* 59 (1989) 124–137.

12. I. Vardoulakis and E.C. Aifantis, A gradient flow theory of plasticity for granular materials. *Acta Mech*. 87 (1991) 197–217.
13. D. Kolymbas, An outline of hypoplasticity. *Arch. Appl. Mech*. 3 (1991) 143–151.
14. F. Darve, Incrementally non-linear constitutive relationships. In: F. Darve (ed.), *Geomaterials: Constitutive Equations and Modelling*. Amsterdam: Elsevier (1991) pp. 213–237.
15. Y.F. Dafalias, Bounding surface plasticity: I. Mathematical foundation and hypoplasticity. *J. Engng. Mech., ASCE* 112 (1986) 966–987.
16. C. Truesdell and W. Noll, The non-linear field theories of mechanics. In: S. Flügge (ed.), *Encyclopedia of Physics* III/c. Heidelberg: Springer press (1965) pp. 1–602.
17. D. Kolymbas, A generalized hypoelastic constitutive law. *Proc. 11th Int. Conf. Soil Mechanics and Foundation Engineering* 5. Rotterdam: Balkema (1988) p. 2626.
18. W. Wu and E. Bauer, A simple hypoplastic constitutive model for sand. *Int. J. Num. Anal. Methods Geomech.* 18 (1994) 833–862.
19. G. Gudehus, A comprehensive constitutive equation for granular materials. *Soils and Foundations* 36 (1996) 1–12.
20. E. Bauer, Calibration of a comprehensive hypoplastic model for granular materials. *Soils and Foundations* 36 (1996) 13–26.
21. P.A. von Wolffersdorff, A hypoplastic relation for granular materials with a predefined limit state surface. *Mech. Cohesive-Frictional Materials* 1 (1996) 251–271.
22. W. Wu and D. Kolymbas, Hypoplasticity then and now. In: D. Kolymbas (ed.), *Constitutive Modelling of Granular Materials*. Berlin, Heidelberg, Newyork: Springer (2000) pp. 57–105.
23. C. Tamagnini, G. Viggiani and R. Chambon, A review of two different approaches to hypoplasticity. In: D. Kolymbas (ed.), *Constitutive Modelling of Granular Materials*. Berlin, Heidelberg, Newyork: Springer (2000) pp. 107–145.
24. E. Bauer and I. Herle, Stationary states in hypoplasticity. In: D. Kolymbas (ed.), *Constitutive Modelling of Granular Materials*. Berlin, Heidelberg, Newyork: Springer (2000) pp. 167–192.
25. J. Tejchman and E. Bauer, Numerical simulation of shear band formation with a polar hypoplastic constitutive model. *Comp. Geotech.* 19 (1996) 221–244.
26. G. Gudehus, Shear localization in simple grain skeleton with polar effect. In: T. Adachi, F. Oka and A. Yashima (eds.), *Proc. of the 4th Int. Workshop on Localization and Bifurcation Theory for Soils and Rocks*. Rotterdam: Balkema (1998) pp. 3–10.
27. G. Gudehus, Attractors, percolation thresholds and phase limits of granular soils. In: R.P. Behringer and J.T. Jenkins (eds.), *Powders and Grains*. Rotterdam: Balkema (1997) pp. 169–183.
28. J. Tejchman, Modelling of shear localisation and autogeneous dynamic effects in granular bodies. *Veröffentlichungen des Institutes für Bodenmechanik und Felsmechanik der Universität Fridericiaca in Karlsruhe*, 140 (1997) 353 pp.
29. E. Bauer and W. Huang, Numerical study of polar effects in shear zones. In: G.N. Pande, S. Pietruszczak and H.F. Schweigers (eds.), *Proc. of the 7th Int. Symp. on Num. Models in Geomechanics*. Rotterdam: Balkema (1999) pp. 133–138.
30. J. Tejchman and G. Gudehus, Shearing of a narrow granular layer with polar quantities. *Int. J. Num. Meth. Geomech.* 25 (2001) 1–28.
31. W. Huang, K. Nübel and E. Bauer, Polar extension of a hypoplastic model for granular materials with shear localization. *Mech. Materials* 34 (2002) 563–576.
32. J. Tejchman and I. Herle, A "class A" prediction of the bearing capacity of plane strain footings on sand. *Soils and Foundations* 39 (1999) 47–60.
33. K. Nübel and R. Cudmani, Examples of finite element calculations with the hypoplastic law. In: D. Kolymbas (ed.), *Constitutive Modelling of Granular Materials*. Berlin, Heidelberg, Newyork: Springer (2000) pp. 523–538.
34. E. Bauer and W. Huang, Numerical investigation of strain localization in a hypoplstic Cosserat material under shearing. In: C.S. Desai, T. Kundu, S. Harpalani, D. Contractor and J. Kemeny (eds.), *Proc. of the 10th Int. Conf. on Computer Methods and Advances in Geomechanics*. Rotterdam: Balkema (2001) pp. 525–528.
35. G. Gudehus and K. Nübel, Evolution of shear bands in sand. *Géotechnique* 54 (2004) 187–201.
36. J. Hill, Some symmetrical cavity problems for a hypoplstic granular material. *Q. J. Mech. Appl. Math.* 53 (2000) 111–135.
37. E. Bauer and W. Huang, Evolution of polar quantities in a granular Cosserat material under shearing. In: H.-B. Mühlhaus, A.V. Dyskin and E. Pasternak (eds.), *Proc. 5th Int. Workshop on Bifurcation and Localization Theory in Geomechanics*. Rotterdam: Balkema (2001) pp. 227–238.

38. W. Huang, *Hypoplastic Modelling of Shear Localisation in Granular Materials.* Dissertation. Graz University of Technology, Austria (2000) 107 pp.
39. W. Wu and A. Niemunis, Failure criterion, flow rule and dissipation function derived from hypoplasticity. *Mech. Cohesive-Frictional Materials* 1 (1996) 145–163.
40. W. Wu and E. Bauer, A hypoplastic model for barotropy and pyknotropy of granular soils. In: D. Kolymbas (ed.), *Proc. of the Int. Workshop on Modern Approaches to Plasticity*, Amsterdam Elsevier (1993) pp. 225–245.
41. W. Wu, E. Bauer and D. Kolymbas, Hypoplastic constitutive model with critical state for granular materials. *Mech. Materials* 23 (1996) 45–69.
42. W. Wu, E. Bauer, A. Niemunis and I. Herle, Visco-hypoplastic models for cohesive soils. In: D. Kolymbas (ed.), *Proc. of the Int. Workshop on Modern Approaches to Plasticity*, Amsterdam: Elsevier (1993) pp. 365–383.
43. G. Gudehus, Hypoplastic shear localisation in psammoids and peloids. *2nd Int. Symposium on Continuous and Discontinuous Modelling of Cohesive Frictional Materials*, Publication in print (2004).
44. W. Wu, Rational approach to anisotropy of sand. *Int. J. Num Anal. Methods in Geomech.* 24 (1998) 921–940.
45. E. Bauer, W. Wu and W. Huang, Influence of initially transverse isotropy on shear banding in granular materials. In: J.F. Labuz and A. Arescher (eds.), *Proc. of the Int. Workshop on Bifurcation and Instabilities in Geomechanics*. Rotterdam: Balkema (2003) pp. 161–172.
46. E. Bauer and W. Wu, Extension of Hypoplastic Constitutive Model with Respect to Cohesive Powders. In: H.J. Siriwardane and M.M. Zadan (eds.), *Proc. of the Eighth Intern. Conf. on Computer Methods and Advances in Geomechanics*. Rotterdam: Balkema (1994) pp. 531–536.
47. A. Niemunis and I. Herle, Hypoplastic model for cohesionless soils with elastic strain range. *Mech. Cohesive-Frictional Materials* 2 (1997) 279–299.
48. A.E. Green and P.M. Naghdi, A general Theory of an elastic-plastic continuum. *Arch. Rat. Mech. Anal.* 18 (1965) 251–281.
49. W. Huang and E. Bauer, Numerical investigations of shear localization in a micro-polar hypoplastic material. *Int. J. Num. Anal. Meth. Geomech.* 27 (2003) 325–352.
50. H. Matsuoka and T. Nakai, Stress-strain relationship of soil based on the 'SMP'. *Proc. of Speciality Session 9, IX Int. Conf. Soil Mech. Found. Eng.*, Tokyo (1977) pp. 153–162.
51. E. Bauer, Conditions for embedding Casagrande's critical states into hypoplasticity. *Mech. Cohesive-Frictional Materials* 5 (2000) 125–148.
52. W. Huang, E. Bauer and S. Sloan, Behaviour of interfacial layer along granular soil-structure interfaces. *Struct. Engng. Mech.* 15 (2003) 315–329.
53. G. Gudehus, Forced and spontaneous polarisation in shear zones. In: H.-B. Mühlhaus, A. V. Dyskin and E. Pasternak (eds.), *Proc. 5th Int. Workshop on bifurcation and Localization Theory in Geomechanics*, Rotterdam: Balkema (2001) pp. 45–51.